Michigan State University

Project 2

Alex Dombos, Samuel Lipschutz, Charles Loelius

2/5/14

1 Target Selection

In this case, we consider the setup to be a target of stable ^{58}Ni, in its ground state. We thereby find that we have quantum numbers in the entrance partition corresponding to(assuming neutron/proton scattering):

Table 1.1: Table of Quantum Values

Quantum Number	Value
Mass partition x	T=58,P=1
Charge	28
Spin	0
Parity	+

2 Pointlike and Structured Coulomb Scattering

We would expect,in the absence of any nuclear forces, and for a point like nucleus, we would expect that the proton would have a pure Rutherford cross section.Upon taking into account the finite size of the target, we recognize that there is a perturbation in the distribution of charge, so that the electric potential will switch from a $\frac{1}{r}$ term to a linear term proportional to r. We expect that this should mean that at energies high enough

to probe the structure of the proton-i.e. those that can overcome the coulomb potential to have a reasonably large wavefunction in the vicinity of the proton- there ought to be an increased cross section in the forward direction.

We compare this below to four graphs of the coulomb potential, one pointlike and one with spatial extent, with energies of .1 MeV and 50 MeV.

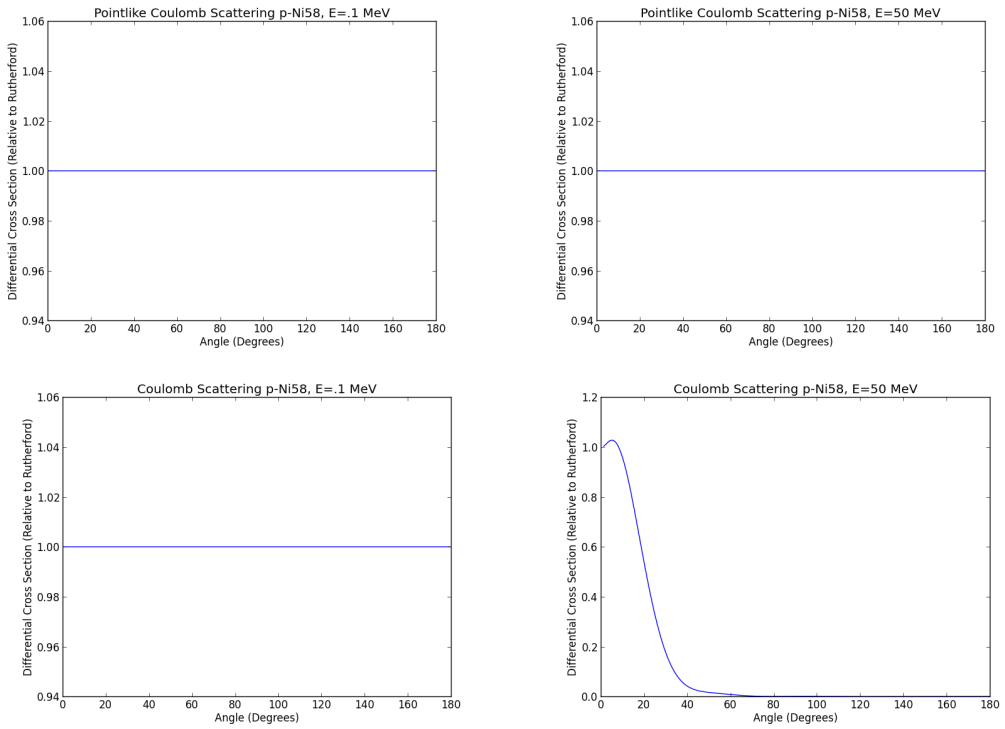

Figure 2.1: Comparison of Pointlike (top) and Extended (bottom) Coulomb Cross Sections

We see that this is exactly what was anticipated, that the pointlike coulomb scattering is indentical to the Rutherford cross section, wheras the case where the target (Nickel 58) has a radial extent shows no structure for low energy projectiles but has the expected forward peaking for high energy.

3 Neutron-Nickel Analysis

3.1 Differential Cross Sections

We then consider the previous analysis using a similar potential model for the nuclear optical potential, but setting the charge of the projectile to 0, and changing the optical potential to be for n-scattering as found at `https://www-nds.iaea.org/cgi-bin/ripl_om_param.pl?Z=28&A=58&ID=1417&E1=0.1&E2=150`. The results of this are plotted below.

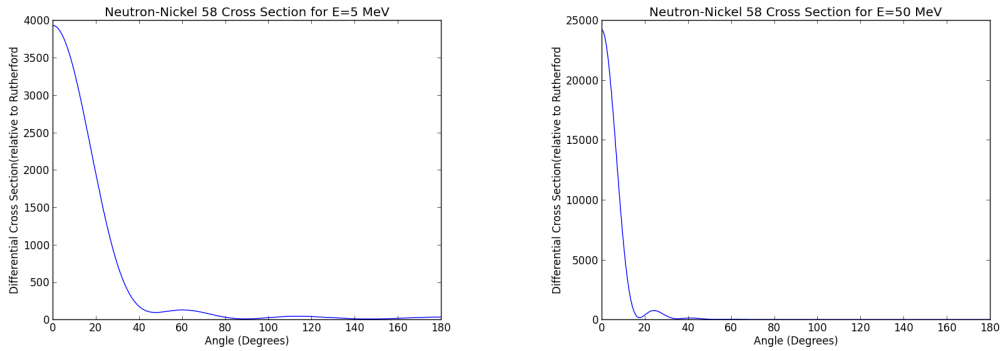

Figure 3.1: Differential Cross Sections for Neutron Interactions

We can see in this case that the distributions are sharply peaked near zero, with the major difference being in the extreme sharpness of the 50 MeV compared to a somewhat broader peak for the 5 MeV. This makes sense because in the absence of a coulomb interaction, the only potential is the optical potential. Since the 50 MeV neutron has a larger energy compared to the optical potential and so is less affected. However, the 5 MeV neutron, no longer prevented from interacting with the optical potential due to the coulomb force, is likely to interact more with the optical potential. This explains the broader scattering. We might expect something similar as energy decreases and the optical potential causes further interactions. However, this must be reconciled with an expected decrease in flux caused by increase interactions with the imaginary potential.

3.2 Increased Diffuseness

In this case, I have set the diffuseness paramaeter to be ten times larger than in the standard found in the previous optical potential. This results in a cross section as follows(for 5 MeV):

We see that for increased diffusiveness that the forward cross section becomes nearly infinite, in comparison to the Rutherford cross section, which follows because at a near infinitely large diffusive constant the potential is nearly zero in any area and so has no

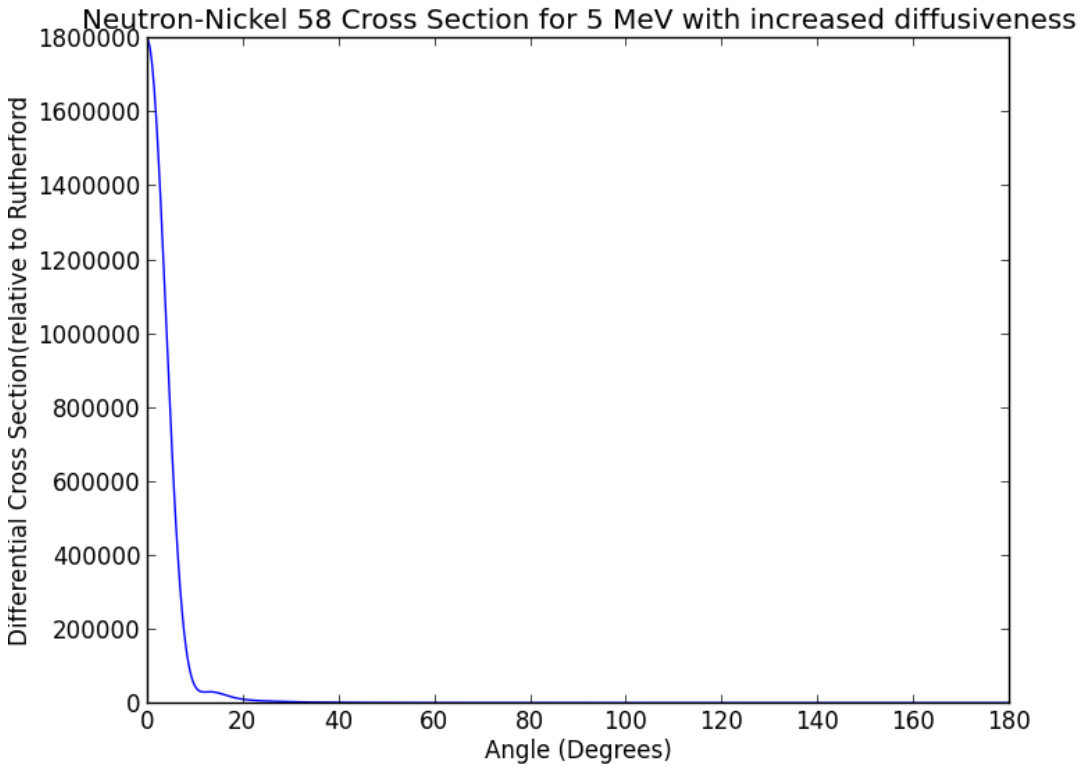

effect on the trajectory. Thus the particle will continue unperturbed, and so have a scattering angle of 0. As such it follows that this will be much larger than the Rutherford cross section which in principle should allow for no such scattering. What's more, the diffuseness means the imaginary potential absorbs less and so the cross section becomes much larger.

3.3 Increased Radius

In this case we consider a radius parameter in the optical potential to also be ten times larger than in the potential defined above. This has the effect of increasing the range over which the potential is strong, and so increases the overall effect of the potential, leaving a larger relative amount of the cross section over which to be scattered. However, it also increases the surface area and volume, which means that there is an increased probability for absorption through the imaginary potential and so an overall smaller cross section.

3.4 Different Strength of Imaginary Potentials

We then ought to anticipate a difference in the total cross sections and so the elastic differential cross sections of the potential, and so a strong imaginary potential(in this

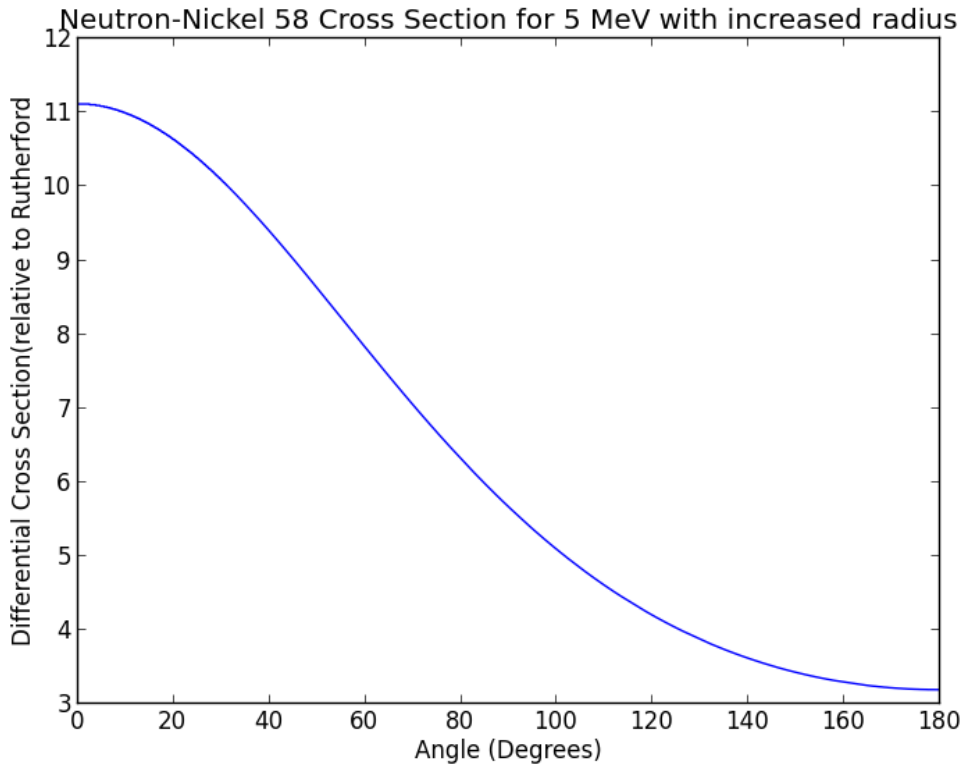

case multiplied by ten from the above) ought to have a much smaller cross section than that of the weak potential(in this case wth the strength of the imaginary potentials divided by ten.)
These are plotted below:

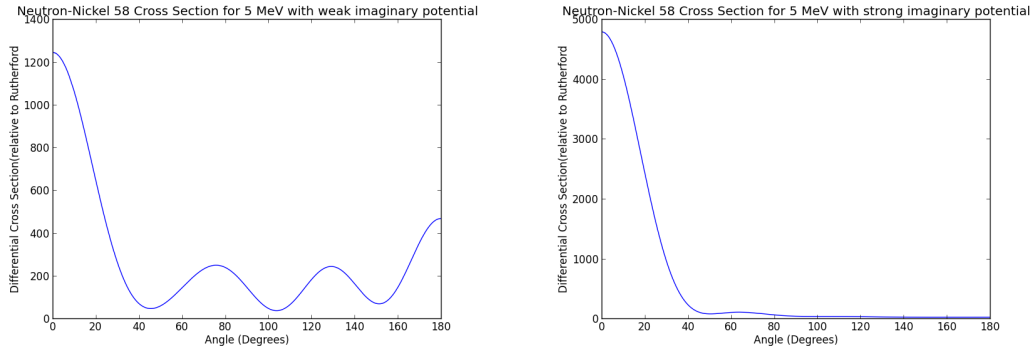

Figure 3.2: Differential Cross Sections for Neutron-Ni58 with Varying Imaginary Potentials

We note that in this instance we don't seem to have the same agreement expected, as it would appear that there is a larger cross section with the strong imaginary potential. However, instead we should look at the modul of the S matricesi for different L states, which will show the overall absorption. These are plotted below:

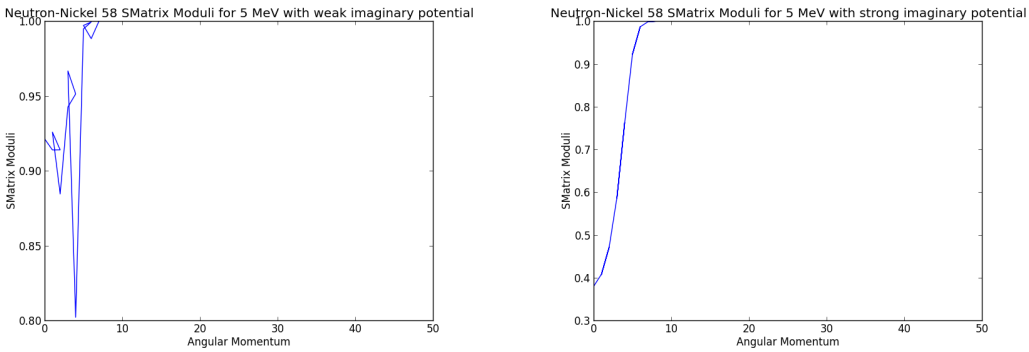

Figure 3.3: Moduli of S for Neutron-Ni58 with Varying Imaginary Potentials

Here we see clearly that especially at low angular momenta the strong imagnary potential starts with a much smaller S matrix than that of the weak, and only slowly converges to 1 with a large L.